

A Rapidly Assembled ZnS-AB Electrochemical Sensor with Enhanced Performance for Luteolin Determination

Jiaoyang Xu^a, Qingtong Li^a, Haifei Yu^a, Wenrui Bi^a, Xinyue Niu^{a, c}, Rong Yuan^a, Nannan Huang^a, Chunjing Zhang^{a, *}, and Haijun Pang^b

^aCollege of Pharmaceutical Sciences, Heilongjiang University of Chinese Medicine, Harbin 150040, P. R. China

^bSchool of Materials Science and Chemical Engineering, Harbin University of Science and Technology, Harbin 150040, China.

^cPharmacy Department, Third Hospital of Heilongjiang, Beian 164000, P. R. China

*To whom correspondence should be addressed.

E-mail: zhangcj922@163.com (C.J. Zhang).

Section 1 Additional Experimental Section

I. Characterization and Electrochemical Testing Methods

All the electrochemical tests were carried out in a three-electrode testing system (CHI760E electrochemical workstation, Chenhua, Shanghai), where the glassy carbon electrode (3.0 mm in diameter) as a working electrode, a commercial Ag/AgCl (3.0 M KCl) as reference electrode and platinum wire as counter electrode. The FT-IR spectra were obtained with a Bruker Tensor II spectrometer (Bruker, Germany). The surface structures and morphology of the samples were characterized by a field-emission scanning electron microscopy (FE-SEM) (Hitachi, SU8000) and Transmission Electron Microscopy (TEM) (JEOL, JEM-2010200 kV). X-ray photoelectron spectroscopy (XPS) was obtained with Thermo Scientific K-Alpha XPS spectrometer

II. Chemicals and Materials

All reagents utilized for synthesis were procured commercially and are suitable for use without further purification. Na_2SO_4 (99%) and $\text{Zn}(\text{CH}_3\text{COO})_2 \cdot 2\text{H}_2\text{O}$ (99%) were purchased from Tianjin Dongli District Tianda Chemical Reagent Factory, KCl (99.5%), disodium hydrogen phosphate ($\text{Na}_2\text{HPO}_4 \cdot 12\text{H}_2\text{O}$, 99%) were purchased from Tianjin Tianli Chemical Reagent Co., Ltd., potassium ferrocyanide (99.5%) was purchased from Tianjin Zhiyuan Chemical Reagent Co., Ltd., potassium ferrocyanide (99.5%) was purchased from Tianjin Hengxing Chemical Reagent Manufacturing Co., Ltd., sodium dihydrogen phosphate ($\text{NaH}_2\text{PO}_4 \cdot 2\text{H}_2\text{O}$, 99%) was purchased from Tianjin Kaitong Chemical Reagent Co., Ltd., acetylene black (AB), sodium hydroxide (NaOH, 96%), sodium citrate (SC, 98%), β - D-glucose (GLU), ascorbic acid (AA), apigenin (API, 98%), DL arginine (ALA, 99%), quercetin (QU, 95%) and L-isoleucine (ILE, 99%) were purchased from Aladdin, anhydrous ethanol ($\text{C}_2\text{H}_6\text{O}$, 99.7%), thiourea (99%), kaempferol (KAE, 97%), and L-methionine (MET, 99%) were purchased from Rohan, and morin (MR) was purchased from Shanghai McLean Biochemical

Technology Co., Ltd.

III. General Material characterization and electrochemical test methods

The differential pulse voltammetry (DPV), cyclic voltammetry (CV) and electrochemical impedance spectroscopy (EIS) were performed with a CHI-760E electrochemical workstation (Shanghai ChenHua Instruments Co, China). A conventional three-electrode system was employed for the electrochemical detection, which was composed of a modified glass carbon electrode (GCE, 3 mm in diameter) as the working electrode, a platinum wire electrode as the counter electrode, and Ag/AgCl (3.0 M KCl) as the reference electrode.

IV. Detailed calculation process of electroactive surface area for the ZnS-AB composite

This was done as follows: ZnS-AB/GCE was immersed into 10 mL of a mixed solution containing 0.005 M $[\text{Fe}(\text{CN})_6]^{3-/4-}$ and 0.1 M KCl, and the scanning potential was set in the range of -0.1 - 0.6 V, and the scanning rate in the range of 0.01 V/s - 0.1 V/s. Based on the linear equation $I_{\text{pa}} = 511.400 v^{1/2} + 17.766$ ($R^2 = 0.998$), the effective surface area of the ZnS-AB composite is determined using the Randles-Sevcik equation (Eq 1) [1, 2].

$$I_{\text{pa}} = 2.69 \times 10^5 n^{3/2} A_{\text{eff}} D_0^{1/2} C v^{1/2} \quad (1)$$

In the formula, I_{pa} represents the peak current at the anodic peak, n is the number of transferred electrons, A_{eff} is the electroactive surface area of the electrode, D_0 is the diffusion coefficient of the $[\text{Fe}(\text{CN})_6]^{3-/4-}$ solution, C is the molar concentration of $[\text{Fe}(\text{CN})_6]^{3-/4-}$ solution, and v is the scanning rate, where the diffusion coefficient of $[\text{Fe}(\text{CN})_6]^{3-/4-}$ solution, $D_0 = 7.6 \times 10^{-6} \text{ cm}^2/\text{s}$, $C = 0.000005 \text{ mol}/\text{cm}^3$, and the number of transferred electrons, $n = 1$, $v^{1/2}$ represents the square root of the scan rate. By substituting these parameters into the equation, The electrically active surface area of ZnS-AB/GCE was obtained as 0.138 cm^2 , which was more than two times higher compared with 0.052 cm^2 of bare GCE

V. Detailed relationship and calculation process of the anodic (E_{pa}) and cathodic (E_{pc}) peaks and the scan rates for of the ZnS-AB composite

The specific operation was as follows: ZnS-AB/GCE was immersed into 0.1 M

PBS at pH 5.0, the scanning potential range was set to 0.1-0.7 V, and the scanning rate was 0.05 V/s. After the baseline of the scan overlaps, add the prepared 25 μ M LU solution and change the scan rates (0.05-0.5 V/s) of the reaction system.

The peak potential increases with the increase of scanning rate, and $\log v$ is linearly related to the peak potential (E_p) with the linear equations : $E_{pa} = 0.056 \log v + 0.504$ ($R^2 = 0.999$), $E_{pc} = -0.062 \log v + 0.277$ ($R^2 = 0.993$). The α and n can be calculated from the experimentally derived $\log v$ versus E_p by means of the Laviron equation ^[3]: (Eq 2 and 3)

$$E_{pa} = E^0 + 2.3 RT \log v / ((1-\alpha)nF) \quad (2)$$

$$E_{pc} = E^0 - 2.3 RT \log v / (\alpha nF) \quad (3)$$

Where α represents the charge transfer coefficient, n represents the number of electrons transferred, E^0 represents the standard potential, v represents the scan rate, R , T , and F are constants ($R = 8.314 \text{ J/(K}\cdot\text{mol)}$, $T = 298 \text{ K}$, $F = 96485 \text{ C/mol}$). The surface coverage of LU on ZnS-AB/GCE can be calculated according to the equation: $I_{pa} = n^2 F^2 v A \Gamma / 4RT$, where Γ represents the surface aggregation concentration of the electroactive substance, and n represents the number of electron transfers, and the above calculations result in $n \approx 2$ and F denotes the Faraday constant, v represents the scan rate, A represents the electroactive surface area of ZnS-AB/GCE, which was derived in section 3.3.5 above as $A = 0.138 \text{ cm}^2$, $R = 8.314 \text{ J/(K}\cdot\text{mol)}$, representing the gas constant, $T = 298 \text{ K}$, representing the temperature, according to the above formula, it is calculated that $\Gamma = 2.386 \times 10^{-10} \text{ mol/cm}^2$.

VI. Experimental method

Catalytic performance

This was done as follows: the modified electrode was immersed in 0.1 M pH 5.0 PBS, the scanning potential range was set from 0.1 to 0.7 V and the scanning rate was 0.05 V/s.

Electrochemical impedance of composite electrodes

This was done as follows: the modified electrode was immersed into 10 mL of a mixed solution containing 0.005 M $[\text{Fe}(\text{CN})_6]^{3-/4-}$ and 0.1 M KCl, and the impedance

frequency range of 0.01 Hz - 10^4 Hz was set to carry out impedance experiments of different modified electrodes.

Linear range and detection limit

This was done as follows: by immersing ZnS-AB/GCE into 10 mL of 0.1 M PBS of pH 5.0, setting the scanning potential range from 0.1-0.7 V, and then adding different concentrations of LU solution sequentially after the baseline was rejoined, and recording the value of the current generated each time and the concentration of the reaction system at that time.

This sensor exhibits significant multi-segment linear response characteristics within different concentration ranges. We discuss attributioning this to the adsorption kinetics on the electrode surface and the saturation effect of the active site: In the presence of extremely low analyte concentrations, the electrode surface possesses a large number of unoccupied active sites. Analyte molecules can freely diffuse and adsorb onto these sites, undergoing rapid and efficient electrochemical reactions. At this stage, the current response (I) is directly proportional to the analyte concentration (C), and the reaction rate is dominated by the mass transfer process (diffusion), resulting in a steep linear increase. When the analyte concentration exceeds the first turning point $0.21\text{ }\mu\text{M}$, the limited availability of active sites becomes the key constraint governing the response characteristics. In the medium concentration range ($0.21\text{-}3.7\text{ }\mu\text{M}$), the reaction mechanism gradually shifts from diffusion dominance to adsorption kinetic control. The reduction in available active sites leads to a slowdown in the increase of the response. In the high concentration range ($3.7\text{-}28\text{ }\mu\text{M}$), the electrode surface approaches saturation coverage, and the reaction rate becomes entirely determined by the intrinsic kinetics of the surface reaction or the product desorption step. The response enters a quasi-platform linear region with minimal growth, indicating that the sensor has reached its maximum response capacity. Therefore, lower slope values are obtained in the second and third linear ranges. Such a phenomenon is consistent with literature reports on sensitivity attenuation due to limited active sites [4-7].

Real sample analysis

The *Lonicera japonica* sample was ground into powder form, the *Lonicera*

japonica powder sample was taken and weighed, 50 mL of 70 % ethanol was added, weighed, ultrasonicated for 1 h, cooled to room temperature, weighed again, and the lost weight was made up with 70 % ethanol, shaken well, filtered, and the renewed filtrate was collected as the stock solution of *Lonicera japonica* sample, which was then diluted with 0.1 M pH 5.0 PBS as a buffer solution for the real sample. Rat serum was diluted with 0.1 M pH 5.0 PBS as a buffer solution for authentic samples.

Section 2 Additional images and textures

I \square PXR D patterns of ZnS, AB, ZnS-AB

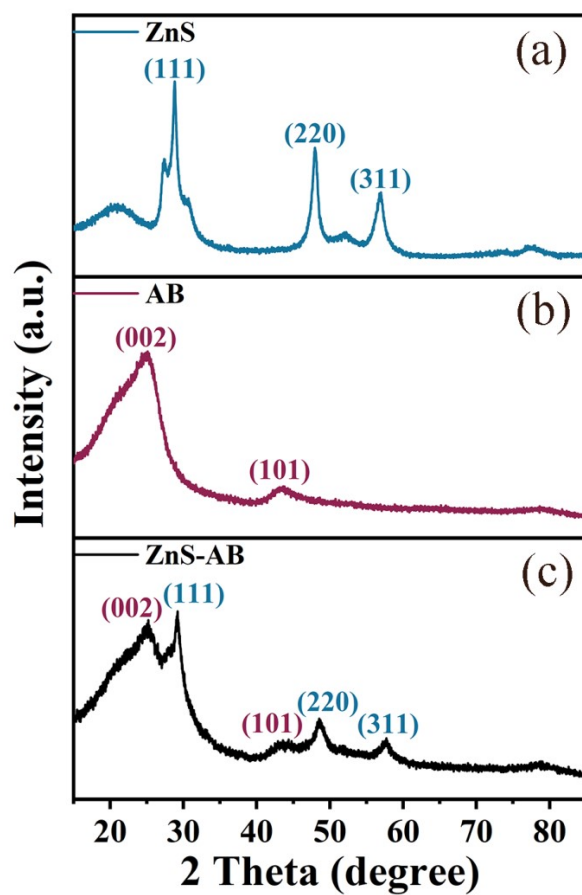


Fig. S1 The PXR D patterns of ZnS, AB, ZnS-AB.

II \square The FT-IR spectra of ZnS, AB, ZnS-AB

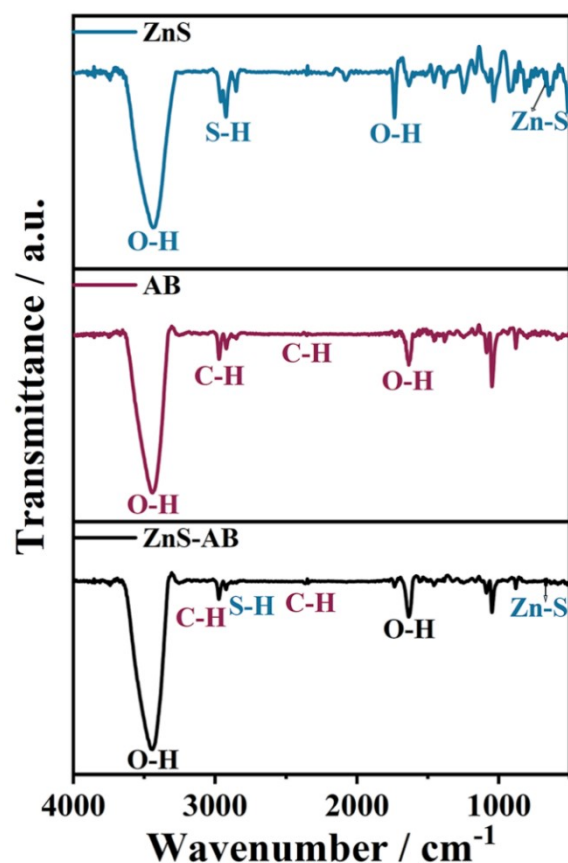


Fig. S2 The FT-IR spectra of ZnS, AB, ZnS-AB.

III □ Surface morphology and structure analysis

Fig. S3 shows the HRTEM image of the ZnS-AB composite. The lattice spacings measured for AB are 0.34 nm, 0.35 nm, and 0.35 nm, all of which correspond to the (002) plane of AB as compared with the JCPDS standard card. Similarly, the lattice spacings calculated for ZnS are 0.30 nm, 0.30 nm, and 0.31 nm, matching the (111) plane of ZnS based on the JCPDS standard. Together, these findings not only confirm once again the successful synthesis of ZnS-AB, but also provide further evidence that the composite consists of zinc sulfide encapsulated by AB.

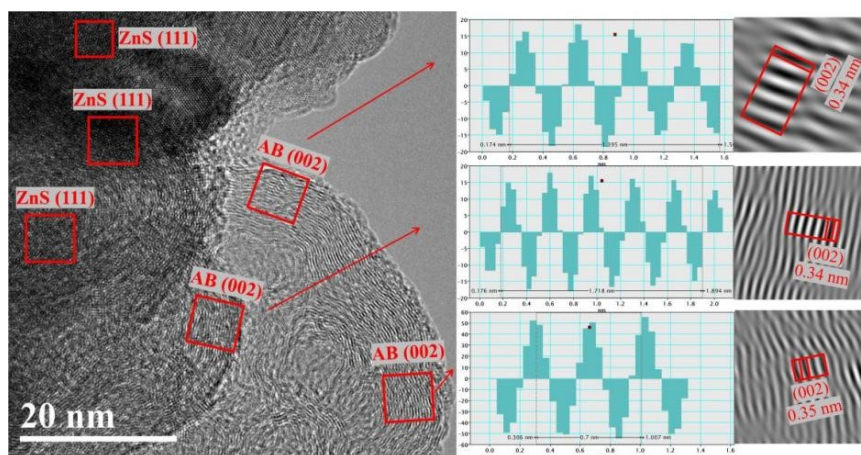


Fig. S3 The HRTEM images of ZnS-AB.

IV □ The impact of changes in component ratios

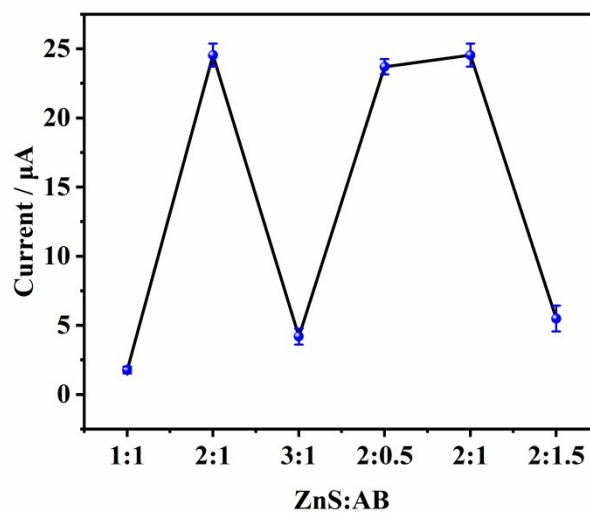


Fig. S4 The Influence of Component Ratio Changes on Peak Response Current. Data are presented as mean \pm SD ($n = 3$).

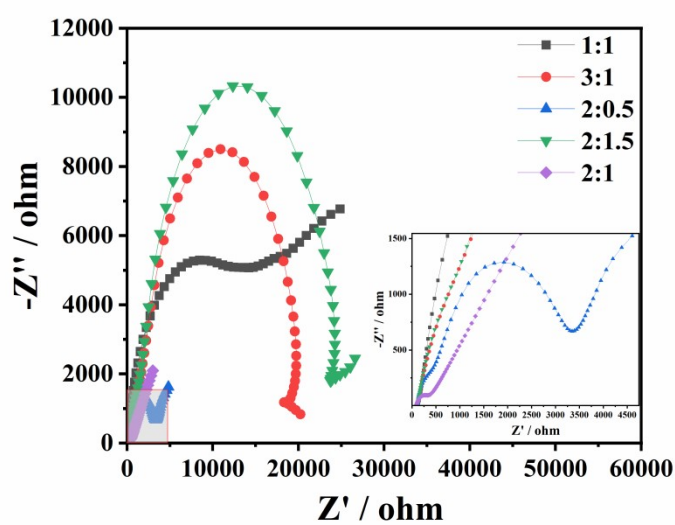


Fig. S5 The EIS of Component Ratio Changes.

V □ *Mechanism diagram of oxidation reaction of Lu on ZnS-AB/GCE surface*

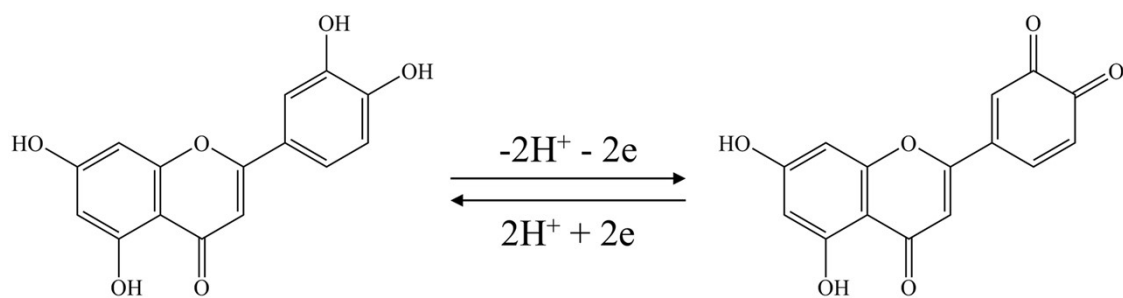


Fig. S6 Mechanism diagram of oxidation reaction of Lu on ZnS-AB/GCE surface.

Section 3 Additional References

References

- [1] X. ZHANG, R. LIU. An ultrasensitive electrochemical sensor for the simultaneous detection of baicalin and baicalein in pharmaceuticals and serum samples. *Talanta*. 2025, 285: 127414.
- [2] A. SELVAM, G. MEENAKUMARI GOPAKUMAR, C. Y. KUO, et al. Design of an ultrasensitive electrochemical sensor using a carbon black/zinc-organic framework nanocomposite for quantifying quercetin in fruits. *Food Chem*. 2025, 491: 145222.
- [3] E. LAVIRON. General expression of the linear potential sweep voltammogram in the case of diffusionless electrochemical systems. *Journal of Electroanalytical Chemistry*, 1979, 101(1): 19-28.
- [4] T. TABANLİGİL CALAM, G. TAŞKIN ÇAKICI. Optimization of square wave voltammetry parameters by response surface methodology for the determination of Sunset yellow using an electrochemical sensor based on Purpald®. *Food Chem*, 2023, 404(Pt A): 134412.
- [5] M. JELVEHZADEH, K. GHANBARI, M. ZAHEDI-TABRIZI. Molecularly imprinted electrochemical sensor based on copper 4-amino benzoic acid metal-organic framework for determination of pregabalin: electrochemical and DFT studies. *Sci Rep*, 2025, 15(1): 37594.
- [6] M. TOHIDINIA, A. BIABANGARD, M. NOROOZIFAR. Platinized agarose microspheres as a new modifier in graphite paste electrodes for the electrochemical determination of 4-aminophenol. *RSC Adv*, 2020, 10(5): 2944-51.
- [7] M. MADEJ, D. MATOGA, K. SKAŻNIK, et al. A voltammetric sensor based on mixed proton-electron conducting composite including metal-organic framework JUK-2 for determination of citalopram. *Mikrochim Acta*, 2021, 188(6): 184.